

See discussions, stats, and author profiles for this publication at: <https://www.researchgate.net/publication/231395214>

# Emission of a Bichromophoric Molecule in the Presence of an Added Quencher. Study of the Time-Resolved Fluorescence by Global Compartmental Analysis with and without the Use of a M...

ARTICLE *in* THE JOURNAL OF PHYSICAL CHEMISTRY · JUNE 1995

Impact Factor: 2.78 · DOI: 10.1021/j100023a014

---

CITATIONS

7

---

READS

7

## 5 AUTHORS, INCLUDING:



[Jan van Stam](#)

Karlstads universitet

68 PUBLICATIONS 1,496 CITATIONS

SEE PROFILE



[Klaas A Zachariasse](#)

Max Planck Institute for Biophysical Chemistry

125 PUBLICATIONS 4,830 CITATIONS

SEE PROFILE



[Frans C De Schryver](#)

University of Leuven

673 PUBLICATIONS 21,484 CITATIONS

SEE PROFILE

# Emission of a Bichromophoric Molecule in the Presence of an Added Quencher. Study of the Time-Resolved Fluorescence by Global Compartmental Analysis with and without the Use of a Model Compound

Jan van Stam, Luc Van Dommelen, Noël Boens,\* Klaas Zachariasse,<sup>†</sup> and Frans C. De Schryver\*

Department of Chemistry, Katholieke Universiteit Leuven, Celestijnenlaan 200 F, B-3001 Heverlee, Belgium

Received: October 6, 1994; In Final Form: March 16, 1995<sup>®</sup>

The previously presented bicompartamental models for intramolecular excited-state systems with added quencher [Boens et al. *J. Phys. Chem.* **1993**, 97, 799 and Van Dommelen et al. *J. Phys. Chem.* **1993**, 97, 11738] are experimentally investigated by time-resolved fluorescence measurements. The emission of the bichromophore bis(2-pyrenecarboxylic acid) 1,6-hexanediyl ester was studied in the absence and presence of iodomethane as a fluorescence quencher. Two different approaches are examined: one where no information is known beforehand and another where the time-resolved emission from the model compound hexyl 2-pyrenecarboxylate was used in the fittings. In the first approach, it was possible to obtain upper and lower limits for the rate constants  $k_{01}$ ,  $k_{21}$ ,  $k_{02}$ , and  $k_{12}$  (see Scheme 1) by analyzing at different preset values of the rate constant  $k_{01}$ . For the other approach, the parameter values of  $k_{01}$  and  $k_{Q1}$  were defined by linking these parameters with the corresponding rate constants of the model compound, whose quenched decays were included in the data analysis. For the calculations of the species-associated emission spectra (SAEMS) two different strategies were followed in the data analysis: one where no information from the model compound steady-state fluorescence spectra was included and one which made use of such information. SAEMS were obtained for both strategies, but inclusion of the steady-state fluorescence spectra information leads to better defined SAEMS for the locally excited state and excimer emissions.

## 1. Introduction

Lately, the family of models used to interpret fluorescence decay data has been extended by the introduction of the compartmental model, where the system investigated is described as consisting of different kinetically distinguishable compartments. Theory and experimental results for intermolecular excited-state processes have been presented,<sup>1–4</sup> as well as for intramolecular excited-state processes.<sup>5–9</sup> It is well-known that the global analysis method,<sup>10,11</sup> i.e., when data from several different experiments are analyzed simultaneously with common model parameters partly or totally linked, is generally superior to single-curve analysis. Data from time-resolved fluorescence measurements are well suited for global analysis, a method that has been much used in this field since its introduction.<sup>11–13</sup> As the compartmental model relies on relations between experiments performed under different conditions, it is by definition a global model.

In the cases where compartmental analysis is suitable, the model allows for direct determination of the rate constants and the spectral absorption and emission parameters, describing the system. In preceding articles concerning intramolecular excited-state processes in bicompartamental systems, special interest has been focused on the identifiability problem in the absence<sup>5</sup> and presence<sup>6</sup> of an added fluorescence quencher, as well as on the possibilities to determine the upper and lower limits for the rate constants through the so-called *scanning* technique,<sup>7,8</sup> and on the calculation of the species-associated emission (SAEMS)<sup>8,14</sup> and excitation (SAEXS)<sup>8</sup> spectra.

For *intramolecular* two-state excited state processes, it was shown that when the fluorescence decay is monitored in the

presence of an added quencher at at least three quencher concentrations (one of them may be equal to zero), only one system parameter has to be known *a priori*.<sup>6</sup> One requirement is that the two rate constants of quenching for the two excited states be different. For systems with an added fluorescence quencher the scanning procedure can be used to specify the upper and lower limits on the rate constants even if no *a priori* information is available.

It was also shown<sup>8</sup> that any compound with a fluorescence decay rate constant within the upper and lower limits, as calculated from the results obtained by scanning, and with adequate spectral characteristics may serve as a model compound, as its decay will be compatible with the fluorescence kinetic data collected for the bicompartamental system.

This paper reports on the results of time-resolved fluorescence measurements of an intramolecular system with two excited states. The main purpose is to demonstrate how the previously presented models<sup>5–9</sup> can be applied to experimental data. For this purpose, the locally excited state and excimer emissions from bis(2-pyrenecarboxylic acid) 1,6-hexanediyl ester in the absence and presence of the added quencher iodomethane are investigated by the bicompartamental model. The use of a model compound, hexyl 2-pyrenecarboxylate, in the evaluations to obtain *a priori* information is discussed. The photophysics of this and similar bichromophoric compounds has previously been studied and evaluated by the use of a sum of exponentials as model function.<sup>15</sup> For the use of the bicompartamental model, two approaches will be discussed: the approach in which no *a priori* information is assumed and that in which some of the fitting parameters are assumed to be known, e.g., as determined from the model compound hexyl 2-pyrenecarboxylate.

## 2. Experimental Section

**2.1. Chemicals and Solutions.** The bichromophore bis(2-pyrenecarboxylic acid) 1,6-hexanediyl ester (2PC(6)2PC) and

\* To whom correspondence should be addressed.

<sup>†</sup> Max-Planck-Institut für biophysikalische Chemie, Spektroskopie und Photochemische Kinetik, Postfach 2841, D-37018 Göttingen, Germany.

<sup>®</sup> Abstract published in *Advance ACS Abstracts*, May 15, 1995.

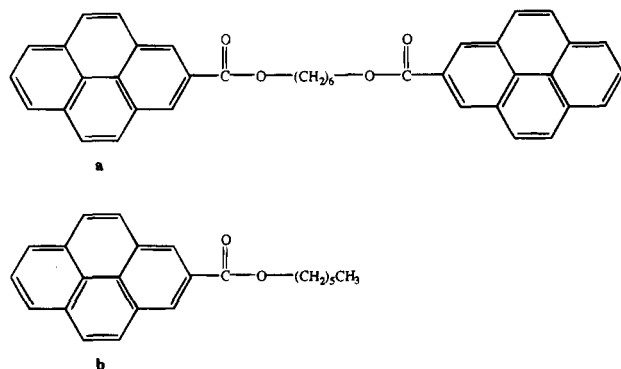


**Figure 1.** Compounds used in this study: (a) bis(2-pyrenecarboxylic acid) 1,6-hexanediyl ester (2PC(6)2PC); (b) hexyl 2-pyrenecarboxylate (2PC(6)).

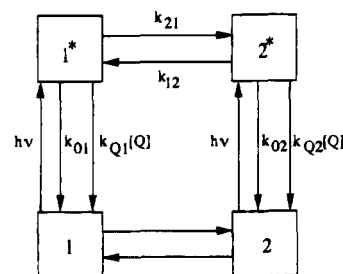
the model compound hexyl 2-pyrenecarboxylate (2PC(6)), shown in Figure 1, were synthesized as described elsewhere.<sup>16</sup> Both 2PC(6)2PC and 2PC(6) were purified by HPLC, performed on equipment from Spectra-Physics (SP8800/8810 LC pump and SP8490 detector). A 25/75 (2PC(6)2PC) or a 5/95 (2PC(6)) mixture (v/v) of ethyl acetate from Janssen Chimica and hexane from Aldrich, both used as received, was used as solvent for the HPLC. After removal of the solvent by vacuum line degassing, the purified product was dissolved in spectroscopic grade toluene (Riedel-de-Haën), which was used as received. The absorbance of 2PC(6)2PC and 2PC(6) at 320 nm was adjusted to be 0.2. The quencher, iodomethane, was from Janssen Chimica and was used as received. The various solutions for the fluorescence measurements were prepared by mixing 2PC(6)2PC or 2PC(6) solution with an iodomethane stock solution in toluene. In the case of 2PC(6)2PC, the iodomethane concentrations were 0, 0.1, 0.2, and 0.4 M, whilst in the case of 2PC(6), the iodomethane concentrations were 0, 0.01, 0.05, 0.1, and 0.2 M. All solutions were degassed by five freeze-pump-thaw cycles.

**2.2. Fluorescence Measurements.** Steady-state fluorescence emission spectra were recorded in the right-angle mode on a SPEX Fluorolog 1680 combined with a SPEX Spectroscopy Laboratory Coordinator DM1B (band-pass 2 nm). Time-resolved fluorescence measurements were performed with the equipment described before.<sup>17</sup> The excitation wavelength was 320 nm, and the emission was monitored at several wavelengths between 380 and 580 nm. All fluorescence decay curves were observed at the magic angle (54.7°). They contained about 3500 peak counts in 512 channels of the multichannel analyzer, of which about 450 were used in the fitting calculations, starting from the rising edge. When measuring 2PC(6), the time increments were 35, 290, and 597 ps/channel and the reference compound for convolution<sup>18</sup> was POPOP (solvent = methylcyclohexane, decay time = 1.1 ns) for the two shortest time increments and 9,10-diphenylanthracene (solvent = methanol, decay time = 6.1 ns) for the longest time increment. When measuring 2PC(6)2PC, POPOP was used as reference and the emission was collected at two time increments, 35 and 278 ps/channel. All measurements were performed at 20 °C.

### 3. Theory and Data Analysis

**3.1. Theory.** **3.1.1. Fluorescence Decay Kinetics.** The theory of reversible intramolecular processes in systems with two excited states with added quencher<sup>6</sup> has been presented previously and will only be briefly summarized here. Consider an intramolecular system with two excited states, as given in Scheme 1. The deactivation rates for processes not including fluorescence quenching,  $k_{01}$  and  $k_{02}$ , are the sums of the rate

**SCHEME 1: Schematic Picture of an Intramolecular Bicompartimental System<sup>a</sup>**



<sup>a</sup> Ground-state species 1 and 2 form a reversible equilibrium. Excitation by light creates the excited-state species 1\* and 2\*, which can decay by fluorescence, internal conversion, and intersystem crossing with the composite rate constants  $k_{01}$  and  $k_{02}$ , respectively. The rate constant describing the transformation 1\*  $\rightarrow$  2\* is represented by  $k_{21}$ , whereas  $k_{12}$  characterizes 2\*  $\rightarrow$  1\*. The rate constants for quenching of excited states 1\* and 2\* are represented by  $k_{Q1}$  and  $k_{Q2}$ , respectively.

constants for fluorescence, internal conversion, and intersystem crossing for each state considered. Addition of a quencher Q to the system accelerates the deactivation by  $k_{Qi}[Q][i^*]$ , where  $i^*$  denotes the excited states 1\* or 2\*, respectively. It is assumed that the presence of the quencher does not alter the ground-state equilibrium and that the rate constants of quenching are time independent. The fluorescence decay after  $\delta$ -pulse excitation can be written as a sum of two exponential decays:

$$f(\lambda_{em}, \lambda_{ex}, t) = \alpha_1 \exp(\gamma_1 t) + \alpha_2 \exp(\gamma_2 t), \quad t \geq 0 \quad (1)$$

The exponential factors  $\gamma_i$  are related to the observed decay times  $\tau_i$  according to

$$\gamma_i = -1/\tau_i \quad (2)$$

and are given by

$$\gamma_i = -1/2 \{ S_1 + S_2 + (k_{Q1} + k_{Q2})[Q] \pm \{ (S_1 - S_2 + (k_{Q1} - k_{Q2})[Q])^2 + 4P \}^{1/2} \} \quad (3)$$

with

$$S_1 = k_{01} + k_{21} \quad (4a)$$

$$S_2 = k_{02} + k_{12} \quad (4b)$$

$$P = k_{12}k_{21} \quad (4c)$$

Note that the exponential factors  $\gamma_i$  depend on the rate constants  $k_{ij}$  and  $k_{Qi}$ , as well as on  $[Q]$ . It should be stressed that the exponential factors, or equivalently the decay times, cannot be connected to a specific state; e.g.,  $-1/\gamma_1$  does not correspond to the lifetime of state 1\*. The pre-exponential factors  $\alpha_i$  depend on the rate constants  $k_{ij}$  and  $k_{Qi}$ ,  $[Q]$ , the normalized absorbances  $\tilde{b}_i(\lambda_{ex})$ , and the normalized spectral emission weight-factors  $\tilde{c}_i(\lambda_{em})$ .<sup>1</sup>

**3.1.2. Species-Associated Emission Spectra (SAEMS).** SAEMS<sub>*i*</sub> is the contribution of species  $i^*$  to the total steady-state emission spectrum,  $F_s$ .<sup>1,8</sup>

$$SAEMS_i(\lambda_{em}, \lambda_{ex}) = \Omega_i(\lambda_{em}, \lambda_{ex}) F_s(\lambda_{em}, \lambda_{ex}) \quad (5)$$

with

$$\Omega_i = [\{ \tilde{c}_i(\lambda_{em}) (\mathbf{A}^{-1} \tilde{\mathbf{b}}^{-1}(\lambda_{ex}))_i \} / \{ \tilde{c}(\lambda_{em}) (\mathbf{A}^{-1} \tilde{\mathbf{b}}^{-1}(\lambda_{ex})) \}] \quad (6)$$

where **A** is the compartmental matrix, **b̃** the 2 × 1 vector of normalized absorbances, and **c̃** the 1 × 2 vector of normalized emission weights corresponding to Scheme 1:

$$\mathbf{A} = \begin{bmatrix} -(k_{01} + k_{21} + k_{Q1}[Q]) & k_{12} \\ k_{21} & -(k_{02} + k_{12} + k_{Q2}[Q]) \end{bmatrix} \quad (7a)$$

$$\mathbf{\tilde{b}} = \begin{bmatrix} \tilde{b}_1 \\ 1 - \tilde{b}_1 \end{bmatrix} \quad (7b)$$

$$\mathbf{\tilde{c}} = [\tilde{c}_1 \quad 1 - \tilde{c}_1] \quad (7c)$$

As the calculation of  $\Omega_i$  involves parameters depending on the excitation wavelength (**b̃**) and the emission wavelength (**c̃**), the resolution of the SAEMS for a given excitation wavelength is determined by the number of emission wavelengths used in the measurements.

**3.1.3. Rate Constant Limits.** From algebra it follows that the rate constants in Scheme 1 have to satisfy the following inequalities:<sup>7,8</sup>

$$0 < k_{01} < S_1 - P/S_2 \quad (8a)$$

$$P/S_2 < k_{21} < S_1 \quad (8b)$$

$$0 < k_{02} < S_2 - P/S_1 \quad (8c)$$

$$P/S_1 < k_{12} < S_2 \quad (8d)$$

By scanning, i.e., keeping one of the rate constants, such as  $k_{01}$ , fixed at different preset values whilst all others are freely adjustable in the analysis, it is possible to determine  $S_1$ ,  $S_2$ , and  $P$ .<sup>7,8</sup> They will appear as plateaus when  $S_1$ ,  $S_2$ , and  $P$  are plotted against the scanned parameter.

**3.2. Data Analysis.** The compartmental model was implemented in the existing general global analysis program,<sup>13</sup> based on Marquardt's algorithm.<sup>19</sup> The fitting parameters were obtained by minimizing the global reduced  $\chi^2$ :

$$\chi^2 = \left[ \sum_x \sum_y \omega_{xy} (h_{xy}^{\text{obs}} - h_{xy}^{\text{calc}})^2 \right] / \nu \quad (9)$$

where  $x$  sums over all experiments and  $y$  over the appropriate channels for each experiment.  $h$  denotes the observed and calculated fluorescence decay histogram values, respectively,  $\omega$  is the statistical weight (a Poisson distribution is assumed), and  $\nu$  represents the degrees of freedom for the entire data surface. The rate constants  $k_{ij}$ , the rate constants for quenching  $k_{Q_i}$ , and the spectral parameters  $\tilde{b}_1$  and  $\tilde{c}_1$  are directly obtained in the fittings, which were judged by their  $\chi^2$  or its corresponding  $Z_{\chi^2}$  values:

$$Z_{\chi^2} = (\chi^2 - 1)(\nu/2)^{1/2} \quad (10)$$

The fit was considered to be good when the global  $Z_{\chi^2} \leq 10$  for the entire data surface (60 different experiments and 28 000 total data points) and when the local  $Z_{\chi^2} \leq 5$  for each individual decay trace. The additional statistical criteria to judge the quality of the fits are described elsewhere.<sup>20</sup> All quoted errors are one standard deviation estimated from the covariance matrix available in the nonlinear least squares analysis. The decay time of the reference compound was held constant at its estimated value during the fittings.

If the determination of the spectral parameters  $\tilde{b}_1$  and  $\tilde{c}_1$  is of interest, the validity of the values for these parameters can only be judged as acceptable if the calculated SAEMS cor-

respond to independently obtained stationary spectral information, e.g., steady-state fluorescence spectra. When the fluorescence spectrum from an appropriate model compound is included, it is assumed that the model compound spectrum is equivalent to that of one of the compartments.

## 4. Results and Discussion

Two different approaches will be discussed: in section 4.1 the data from 2PC(6)2PC will be analyzed under the assumption that no *a priori* information is available, whereas in section 4.2 use will be made of information obtained from the model compound 2PC(6).

Under the conditions in section 4.1, the system is not identifiable<sup>6</sup> and only the upper and lower limits of the rate constants  $k_{01}$ ,  $k_{21}$ ,  $k_{02}$ , and  $k_{12}$  can be specified by scanning the values of one of the rate constants. Under those of section 4.2, however, the system becomes fully identifiable, because the inclusion of the quenched decay of the model compound allows one to assign values to both  $k_{01}$  and  $k_{Q1}$ . For an intramolecular bicompartamental system with added quencher, it has previously been shown<sup>6</sup> that prior knowledge of at least one rate constant used in the fittings is necessary for a complete determination of the system.

For the calculations of the SAEMS, two different strategies were followed for each analytical approach. In the framework of the first, referred to as strategy I, no stationary spectral information from the model compound was included, whilst in the second, henceforth referred to as strategy II, available knowledge about  $\tilde{b}_1$  and  $\tilde{c}_1$ , based on steady-state spectral information of 2PC(6), was used.

**4.1. Scanning One Rate Constant of the Bichromophoric System with Added Quencher.** Assuming no *a priori* knowledge of the system, the choice is to apply the scanning technique to the decay data from the measurements on 2PC(6)2PC. In this method, one of the rate constants  $k_{01}$ ,  $k_{21}$ ,  $k_{02}$ , or  $k_{12}$  is held constant at different preset values, whilst all other parameters are freely adjustable. We have chosen to scan the rate constant  $k_{01}$ , but the choice of the scanned rate constant is quite arbitrary.<sup>7,8</sup> During the scanning, the parameters  $k_{01}$ ,  $k_{21}$ ,  $k_{Q1}$ ,  $k_{02}$ ,  $k_{12}$ ,  $k_{Q2}$ , and  $\tilde{b}_1$  were globally linked over the entire data surface ( $\tilde{b}_1$  is a function of the excitation wavelength only).  $\tilde{c}_1$  was regionally, i.e., not over the whole data surface, linked over the two time increments at equal emission wavelengths ( $\tilde{c}_1$  is a function of the emission wavelength only), whilst  $k_{Q1}$  and  $k_{Q2}$  were regionally linked over experiments with added quencher. For the decays obtained in the absence of added quencher, the version of the compartmental model without quenching was used in the fittings to avoid zero values for some of the rate constants and concentrations.

**4.1.1. Strategy I: Only the Value of the Scanned Rate Constant  $k_{01}$  Held Constant.** Following strategy I, all parameters, except the scanned rate constant  $k_{01}$ , were freely adjustable. The entire data set consists of 60 different experiments monitored at eleven emission wavelengths between 395 and 580 nm and collected at two timing calibrations (35 and 278 ps/channel) with 28 000 total data points. The resulting  $S_1$ ,  $S_2$ ,  $P$  (eqs 4), and  $Z_{\chi^2}$  (eq 10) are graphically shown in Figure 2. The averaged plateau values of  $S_1$ ,  $S_2$ , and  $P$  as well as the calculated upper and lower limits on the rate constants  $k_{01}$ ,  $k_{21}$ ,  $k_{02}$ , and  $k_{12}$  are shown in Table 1a. As can be seen in Figure 2, deviations from the plateaus can be observed for  $k_{01}$  values greater than  $1 \times 10^8 \text{ s}^{-1}$ . Furthermore, constancy of  $Z_{\chi^2}$  is evidently the less sensitive parameter from which to determine the width of the plateau, as has been shown previously with simulated data.<sup>8</sup> The estimated values of the two rate constants,

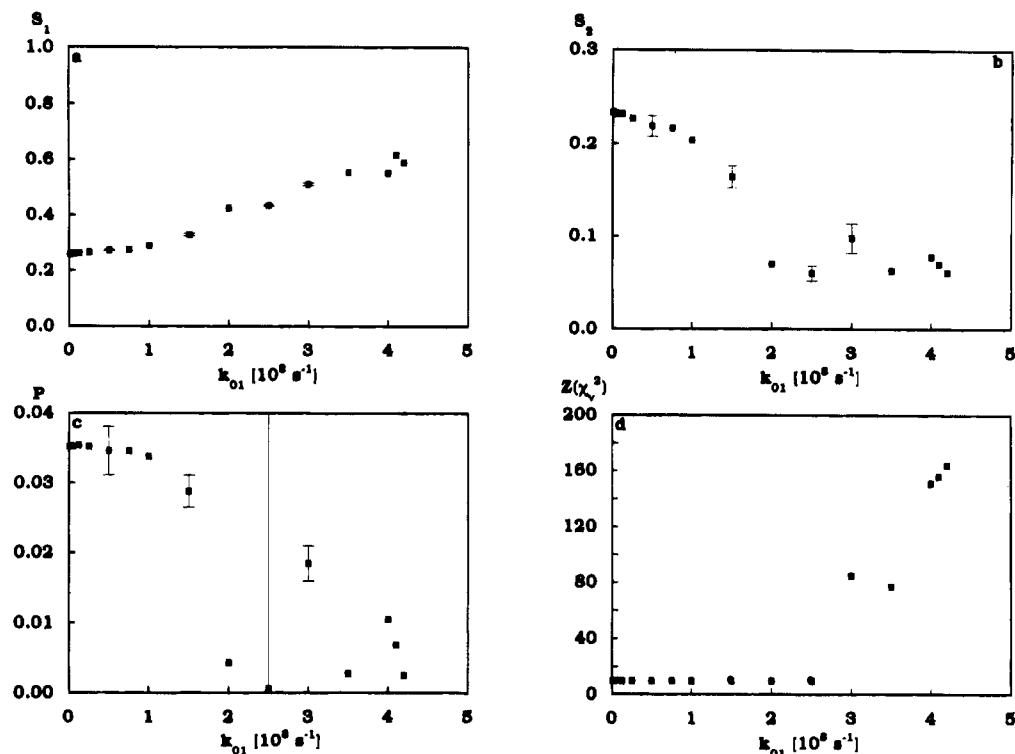


**Figure 2.** (a)  $S_1$ , (b)  $S_2$ , (c)  $P$ , and (d) the global  $Z_{x_2}$  from the scanning following strategy I (see text for details) of the bichromophoric system with added quencher.  $S_1$  and  $S_2$  are given in  $10^9 \text{ s}^{-1}$ ,  $P$  is in  $10^{18} \text{ s}^{-2}$ , and  $Z_{x_2}$  is dimensionless. The standard errors at  $k_{01} = 0.5 \times 10^8$ ,  $1.5 \times 10^8$ ,  $2.5 \times 10^8$ , and  $3.5 \times 10^8 \text{ s}^{-1}$  are shown in parts a–c.

**TABLE 1: Averaged ( $0.001 < k_{01} < 0.075 \text{ ns}^{-1}$ ) Parameters  $S_1$ ,  $S_2$ , and  $P$  as Well as the Calculated Upper and Lower Limits for the Rate Constants  $k_{01}$ ,  $k_{21}$ ,  $k_{02}$ , and  $k_{12}$  Resulting from the Scanning of the 2PC(6)2PC System with Added Quencher Iodomethane<sup>a</sup>**

(a) Strategy I (See Text for Details)

$$S_1 = 0.265 \pm 0.007$$

$$S_2 = 0.227 \pm 0.007$$

$$P = 0.035$$

$$0 < k_{01} < 0.11$$

$$0.15 < k_{21} < 0.26$$

$$0 < k_{02} < 0.10$$

$$0.13 < k_{12} < 0.23$$

(b) Strategy II (See Text for Details)

$$S_1 = 0.249 \pm 0.001$$

$$S_2 = 0.245 \pm 0.008$$

$$P = 0.035$$

$$0 < k_{01} < 0.11$$

$$0.14 < k_{21} < 0.25$$

$$0 < k_{02} < 0.10$$

$$0.14 < k_{12} < 0.24$$

<sup>a</sup>  $S_1$ ,  $S_2$ , and the rate constants are given in  $10^9 \text{ s}^{-1}$ , whilst  $P$  is given in  $10^{18} \text{ s}^{-2}$ .

$k_{Q1}$  and  $k_{Q2}$  are shown in Figure 3a. Note that  $k_{Q1}$  and  $k_{Q2}$  remain constant over a broader range than  $S_1$ ,  $S_2$ , and  $P$ .

From the results obtained by scanning, it is also possible to calculate the SAEMS for each value of  $k_{01}$  where constant values on  $S_1$ ,  $S_2$ , and  $P$  are obtained. The values of  $\tilde{c}_1$  and  $\tilde{b}_1$  necessary for the calculation of  $\Omega_i$  (eq 5) are given for  $k_{01} = 5 \times 10^7 \text{ s}^{-1}$  in Table 2a.  $\Omega_i$  values were calculated as a function of  $k_{01}$  and are graphically shown for two emission wavelengths in Figure 4a.  $\Omega_1$  stays reasonably constant up to  $k_{01} = 1 \times 10^8 \text{ s}^{-1}$  in accordance with Figure 2a.

The SAEMS (eq 7) at  $k_{01} = 5 \times 10^7 \text{ s}^{-1}$  for the locally excited state and excimer emission of 2PC(6)2PC are shown in Figure 4b. In absence of *a priori* information, the obtained spectra are acceptable but show anomalies at shorter wavelengths. On

the basis of the values of  $\tilde{c}_1$  and  $\tilde{b}_1$  (Table 2) and the obtained SAEMS, it follows that the locally excited state is assigned to the first compartment.

**4.1.2. Strategy II: Rate Constant  $k_{01}$  Scanned and  $\tilde{c}_1(395 \text{ nm})$  Held Constant to Unity.** The fluorescence decays of 2PC(6)2PC in the absence of added quencher at various  $\lambda_{\text{em}}$  are shown in Figure 5. The fluorescence decays evolve from a sum of two exponentials at shorter wavelengths (both pre-exponential factors positive) to a difference between two exponentials (one pre-exponential factor positive and the other negative) at longer wavelengths. Note that for all wavelengths the decays are parallel at longer times. It was shown that, if the value of the ratio of the pre-exponential factors for the decays collected in the excimer region differs from negative unity, this indicates the existence of ground-state dimers.<sup>15</sup> This conclusion may only be drawn if the locally excited state emission can be neglected.<sup>15</sup> This condition is fulfilled for 2PC(6)2PC in toluene if the emission is monitored at wavelengths above 530 nm. From the ratio of the pre-exponential factors of the decays at emission wavelengths above 530 nm (some representative samples are shown in Figure 6), it follows that indeed there are preformed dimers in the ground state. For this reason  $\tilde{b}_1$  cannot be held constant at unity but must be treated as a freely adjustable parameter. Furthermore, if one assumes that the emission within the 0,0-band (around 395 nm) solely stems from the locally excited state, the corresponding  $\tilde{c}_1$  can be held constant at unity for all emission wavelengths lower than or equal to 395 nm. This implies that the locally excited state is assigned to compartment 1 as in strategy I.

Including the information  $\tilde{c}_1(395 \text{ nm}) = 1$  and otherwise performing the scanning in the same way as in section 4.2.1, results in the values of  $S_1$ ,  $S_2$ ,  $P$ , and  $Z_{x_2}$  shown in Figure 7 and rate constants for quenching shown in Figure 3b. The range of constant  $k_{Q1}$  values extends up to  $k_{01} = 1 \times 10^8 \text{ s}^{-1}$ . The calculated values of  $\Omega_1$  (Figure 8a) show enhanced stability, compared to those of Figure 4a. This also leads to SAEMS

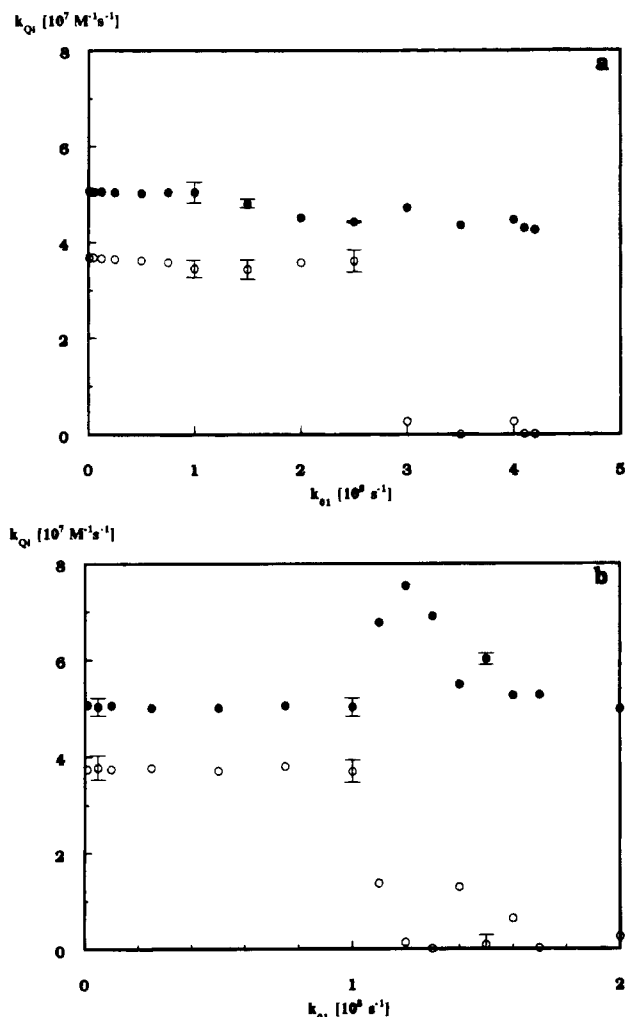


**Figure 3.** Resulting values of the rate constants for quenching,  $k_{Q1}$  (○) and  $k_{Q2}$  (●), when scanning  $k_{01}$  of 2PC(6)2PC with added quencher iodomethane following (a) strategy I (see text for details) and (b) strategy II (see text for details). The standard errors at  $k_{01} = 1.0 \times 10^8$ ,  $1.5 \times 10^8$ , and  $2.5 \times 10^8 \text{ s}^{-1}$  are shown in part a, and those at  $k_{01} = 0.05 \times 10^8$ ,  $1.0 \times 10^8$ , and  $1.5 \times 10^8 \text{ s}^{-1}$  are shown in part b.

**TABLE 2:  $\tilde{\epsilon}_1$  Values Obtained from the Scanning following (a) Strategy I and (b) Strategy II (See Text for Details) of the 2PC(6)2PC Data with Added Quencher Iodomethane at  $k_{01} = 5 \times 10^7 \text{ s}^{-1}$**

$\lambda_{em} \text{ (nm)}$	$\tilde{\epsilon}_1(a)^a$	$\tilde{\epsilon}_1(b)^b$
395	0.865	1 (constant)
400	0.832	$0.953 \pm 0.008$
420	0.683	$0.745 \pm 0.020$
440	0.498	$0.495 \pm 0.005$
460	0.333	$0.278 \pm 0.027$
480	0.224	$0.137 \pm 0.054$
500	0.160	$0.055 \pm 0.062$
520	0.133	$0.022 \pm 0.078$
540	0.121	$0.007 \pm 0.082$
560	0.116	$0.001 \pm 0.083$
580	0.118	$0.003 \pm 0.083$

<sup>a</sup> The estimated value for  $\tilde{\epsilon}_1$  was 0.965. When following strategy I, standard errors were not recovered for all emission wavelengths. <sup>b</sup>  $\tilde{\epsilon}_1$  (395 nm) was held constant at unity. The estimated value for  $\tilde{\epsilon}_1$  was 0.863.

(Figure 8b) which are changed at the short-wavelength side. At shorter wavelengths this is not surprising, as keeping  $\tilde{\epsilon}_1$  (395 nm) constant at unity forces the intensity of the excimer emission in this region of the spectrum to be close to zero. Additionally, at longer wavelengths, i.e.,  $\lambda \geq 520 \text{ nm}$ , the locally

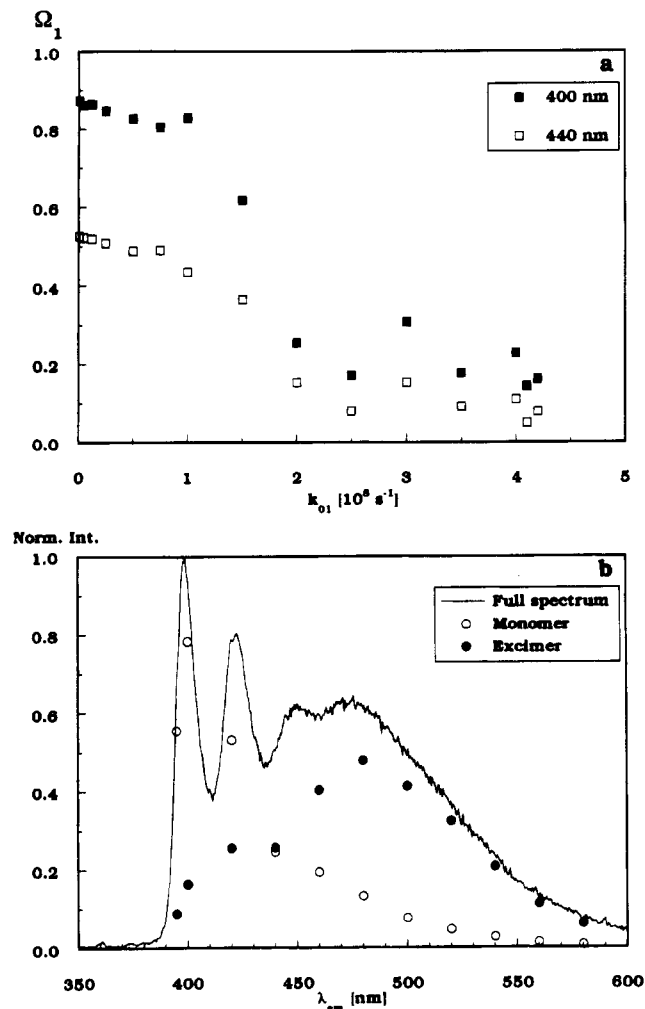


**Figure 4.** (a) Emission weight factor  $\Omega_1$  as a function of the scanned parameter  $k_{01}$  following strategy I (see text for details) from the 2PC(6)2PC system with added quencher at two emission wavelengths (see inserted legend). (b) Calculated SAEMS for locally excited state and excimer emission of 2PC(6)2PC in toluene derived from the scanning following strategy I (see text for details) of the bichromophoric system with added quencher.  $\Omega_{1,2}$  obtained at  $k_{01} = 5 \times 10^7 \text{ s}^{-1}$  were used in the calculations. The SAEMS could be regarded as acceptable under the condition that no model compound is available.

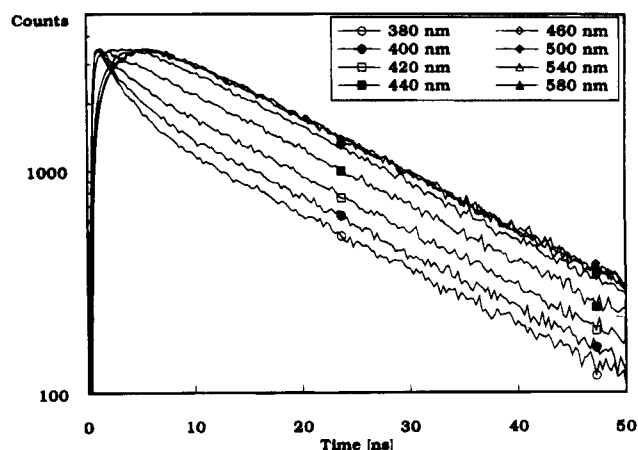


**Figure 5.** Fluorescence decays of 2PC(6)2PC in the toluene in absence of added quencher at various emission wavelengths (see inserted legend).

excited state emission has completely vanished. It is noteworthy that the only difference between strategy I and strategy II is that spectral information is included in the latter:  $\tilde{\epsilon}_1(395 \text{ nm})$

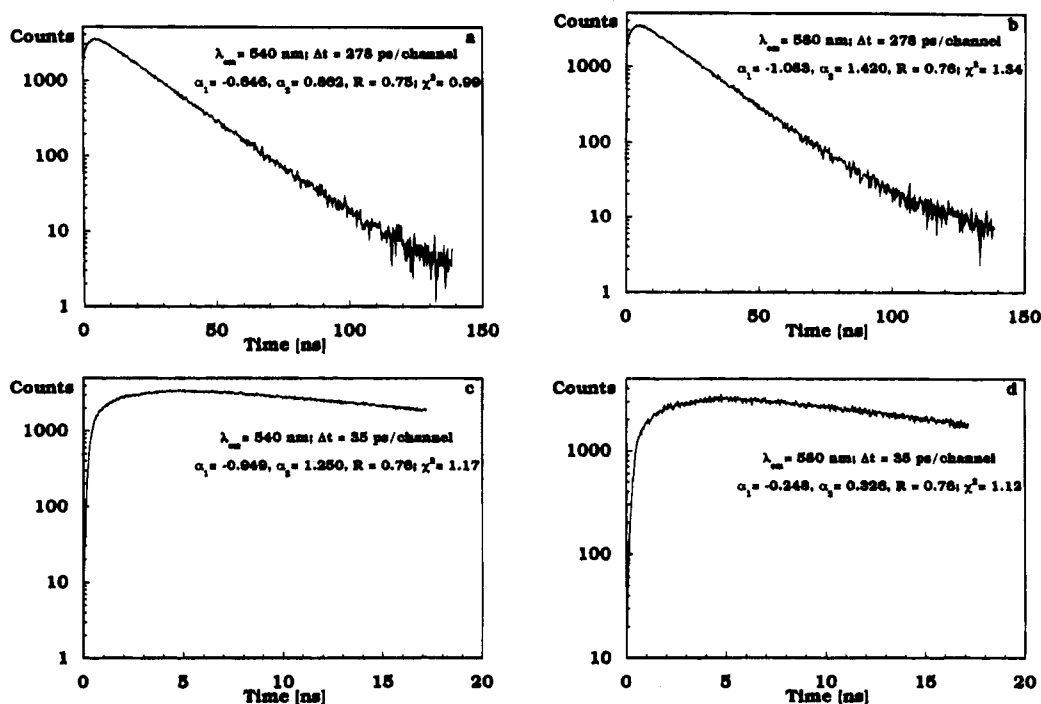


**Figure 6.** Fluorescence decay of 2PC(6)2PC in the absence of added quencher at two different emission wavelengths and two different time increments. Inserted legends give information about emission wavelengths and time increments as well as the pre-exponential factors  $\alpha_i$  obtained (deviation less than 1%), the calculated ratio  $R = |\alpha_1/\alpha_2|$ , and the  $\chi^2$  of the fit. The fits of a biexponential function to the data were performed following the single-curve method with reference deconvolution.

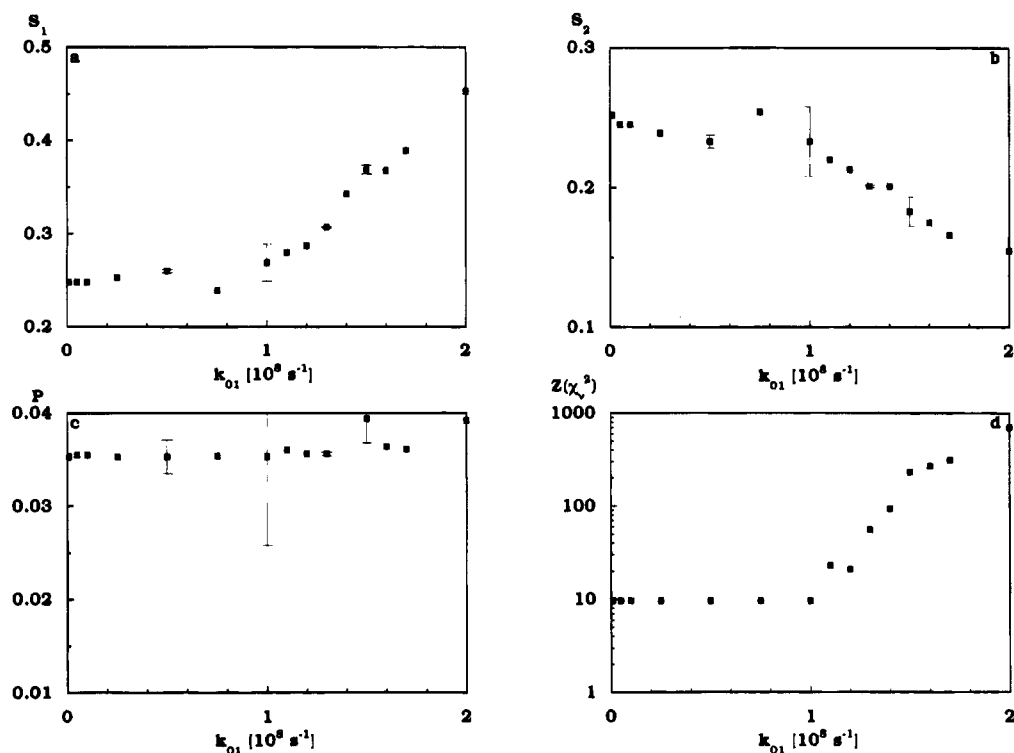


**Figure 7.** Results corresponding to Figure 2 but for strategy II scanings. See text for details. The standard errors at  $k_{01} = 0.5 \times 10^8$ ,  $1.0 \times 10^8$ ,  $1.3 \times 10^8$ , and  $1.5 \times 10^8$  s $^{-1}$  are shown in parts a–c.

is held constant at unity (strategy II) instead of being a freely adjustable parameter (strategy I) in the fittings.

**4.2. Compartmental Model Fitted to the Decay Surface of 2PC(6)2PC with Added Quencher and with the 2PC(6) Data Included in the Surface.** The following step in the data analysis is to fit the compartmental model including quenching to the entire data surface. The decay traces from the 2PC(6) measurements were simultaneously fitted together with the traces from measurements on 2PC(6)2PC with and without added

iodomethane. In this case, one acceptable assumption is that the composite rate constant of deactivation of excited 2PC(6) ( $k_0$  of eq 11) should be the same as that for the locally excited state of 2PC(6)2PC. Assigning the locally excited state to the first compartment as before allows one to link  $k_{01}$  of 2PC(6)-2PC with  $k_0$  of 2PC(6). The fluorescence decays at  $\lambda_{em} = 395$  nm of 2PC(6) at different iodomethane concentrations are shown in Figure 9. To evaluate the decays from 2PC(6), measured at a timing calibration of 597 ps/channel, use was made of eq 11:

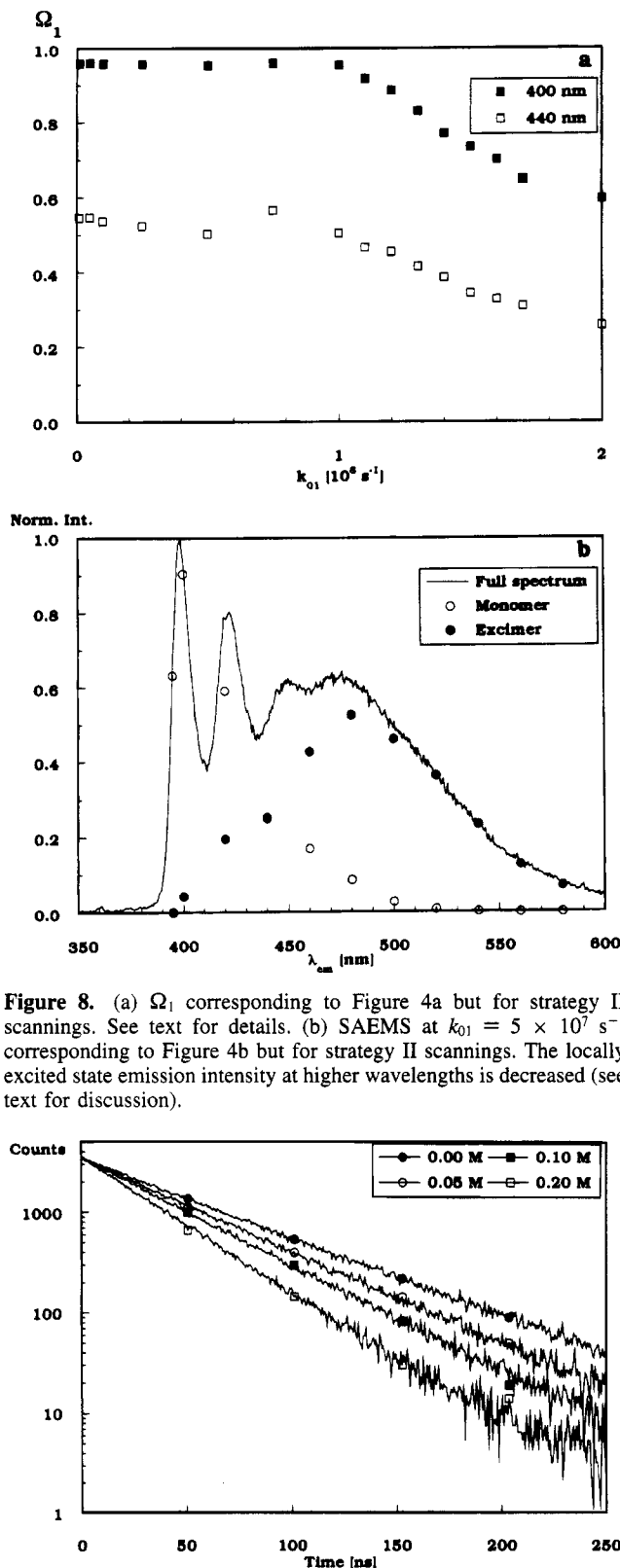


**Figure 8.** (a)  $\Omega_1$  corresponding to Figure 4a but for strategy II scannings. See text for details. (b) SAEMS at  $k_{o1} = 5 \times 10^7$  s $^{-1}$  corresponding to Figure 4b but for strategy II scannings. The locally excited state emission intensity at higher wavelengths is decreased (see text for discussion).

**Figure 9.** Fluorescence decays of 2PC(6) in toluene monitored at 395 nm with various iodomethane concentrations (see inserted legend).

$$f(\lambda_{em}, \lambda_{ex}, t) = f_0 \exp(-\{k_0 + k_q[Q]\}t) \quad (11)$$

where  $f(\lambda_{em}, \lambda_{ex}, t)$  denotes the  $\delta$ -response fluorescence at time  $t$ ,  $f_0$  the  $\delta$ -response fluorescence at time 0,  $k_0$  the first-order decay rate constant, and  $k_q$  the second-order quenching rate constant. A global fit of eq 11 to the data from time-resolved emission measurements on 2PC(6), upon excitation at 320 nm, recorded at 395 and 420 nm, and at four quencher concentrations

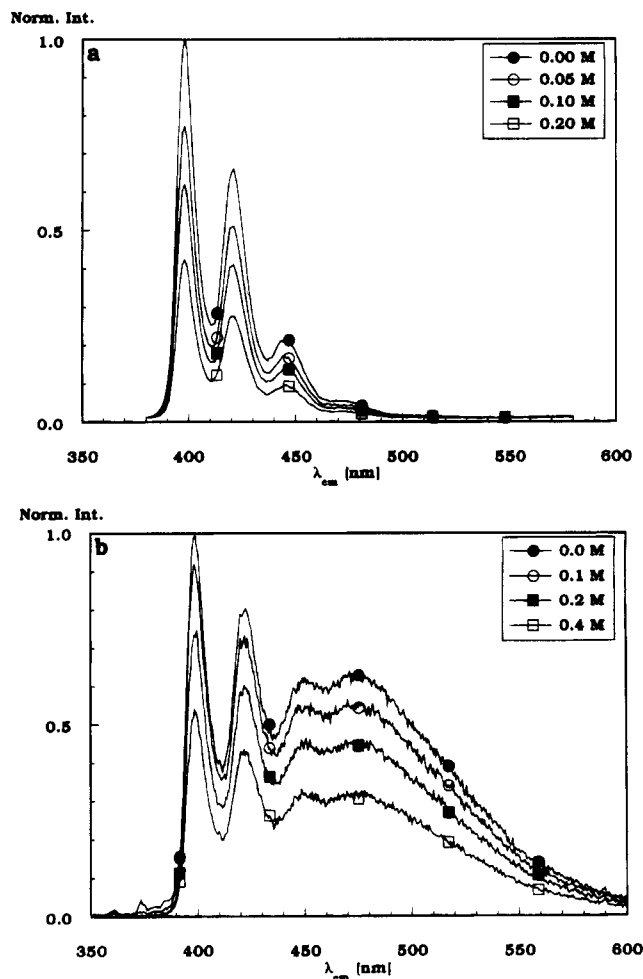


**Figure 10.** Normalized steady-state emission spectra of (a) the model compound and (b) the bichromophore in toluene when excited at  $\lambda_{ex} = 320$  nm at various iodomethane concentrations (see inserted legends).

(0, 0.05, 0.10, and 0.20 M) gave  $k_0 = (1.824 \pm 0.002) \times 10^7$  s $^{-1}$  and  $k_q = (6.69 \pm 0.03) \times 10^7$  M $^{-1}$  s $^{-1}$ . The fits showed excellent statistics: the global and local  $\chi^2$  were all very close to unity.

To check if time-dependent quenching occurs in the studied system,<sup>21</sup> additional fluorescence decays were recorded for 2PC(6) at the same iodomethane concentrations as for the 2PC(6)2PC system (see Experimental Section) at two time increments (35 and 290 ps/channel). These measurements could also be perfectly fitted by eq 11, indicating that under these experimental conditions no corrections for a time-variant quenching rate have to be introduced. The use of a model compound renders the intramolecular bicompartamental system identifiable,<sup>6</sup> making scanning redundant.

The steady-state emission spectra of 2PC(6) and 2PC(6)2PC at excitation wavelength 320 nm and at various quencher concentrations are presented in parts a and b of Figure 10, respectively. When these two spectra are compared, the broad emission band centered at 475 nm is easily identified as the excimer emission from 2PC(6)2PC. The similarity between the 2PC(6) steady-state emission spectrum and the locally excited state emission of 2PC(6)2PC indicates that 2PC(6) fulfills the spectral requirements to be used as a model compound.

Using the stationary spectral information of 2PC(6), it is now possible to re-examine the SAEMS obtained in section 4.1 (Figures 4b and 8b). Following strategy I (Figure 4b) results in a locally excited state emission at too high wavelengths as compared with Figure 10a. Fixing  $\tilde{\epsilon}_1(395$  nm) at unity in the



**TABLE 3: Results from the Global Fit following Strategy I (See Text for Details) of the Compartmental Model including Quenching to Fluorescence Decay Data from 2PC(6)2PC and 2PC(6), Both with and without Added Quencher Iodomethane<sup>a</sup>**

Globally Linked Parameters										
$k_{01}$	$k_{21}$	$k_{Q1}$	$k_{02}$	$k_{12}$	$k_{Q2}$	$\tilde{b}_1$	$S_1$	$S_2$	$P$	$Z_{\chi^2}$
$0.01826 \pm 2 \times 10^{-5}$	$0.28 \pm 0.02$	$0.0665 \pm 3 \times 10^{-4}$	$0.078 \pm 0.004$	$0.12 \pm 0.01$	$0.030 \pm 0.003$	$0.9 \pm 0.1$	0.296	0.196	0.0328	9.85
Regionally Linked Parameters										
$\lambda_{\text{em}}$	$\tilde{c}_1$		$\lambda_{\text{em}}$	$\tilde{c}_1$						
395	$0.83 \pm 0.04$		500	$0.16 \pm 0.07$						
400	$0.81 \pm 0.04$		520	$0.12 \pm 0.08$						
420	$0.69 \pm 0.02$		540	$0.11 \pm 0.08$						
440	$0.523 \pm 0.003$		560	$0.10 \pm 0.09$						
460	$0.36 \pm 0.03$		580	$0.10 \pm 0.09$						
480	$0.23 \pm 0.05$									

<sup>a</sup> The rate constants  $k_{01}$ ,  $k_{21}$ ,  $k_{02}$ , and  $k_{12}$  as well as  $S_1$  and  $S_2$  are given in  $10^9 \text{ s}^{-1}$ , while  $P$  is given in  $10^{18} \text{ s}^{-2}$ . The quenching rate constants  $k_{Q1}$  and  $k_{Q2}$  are given in  $10^9 \text{ M}^{-1} \text{ s}^{-1}$ . 70 files with 32 000 total data points were included in the fittings.  $k_{01}$  and  $k_{Q1}$  were linked with  $k_0$  and  $k_q$ , respectively, for 2PC(6) (eq 11), whose fluorescence decays in the presence and absence of added quencher were included in the fittings. The parameters  $k_{21}$ ,  $k_{02}$ ,  $k_{12}$ ,  $k_{Q2}$ , and  $\tilde{b}_1$  were globally linked over the entire data surface (excluding the part belonging to 2PC(6)), whilst  $\tilde{c}_1$  was regionally linked over the same emission wavelength at different quencher concentrations and different time increments.

analysis (strategy II) results in a better correspondence with the model compound emission (Figures 8b and 10a, respectively).

4.2.1. Strategy I:  $k_{01}$  and  $k_{Q1}$  of 2PC(6)2PC Linked with  $k_0$  and  $k_q$  of 2PC(6), Respectively. The results from the fittings with no steady-state spectral information included are summarized in Table 3. The statistical quality of the fit was excellent, and the results obtained match the upper and lower limits for the rate constants (Table 1a).

The values of the rate constants of quenching estimated by scanning (Figure 3) and the results from the fitting (Table 3) raise a question about the values obtained for the two quenching rate constants. It looks as if  $k_{Q1}$  and  $k_{Q2}$  have interchanged, which might raise doubts about the appropriateness of the model as well as about the fit. It must be emphasized that in the fitting  $k_{Q1}$  is assigned to the locally excited state by linking it with  $k_q$  of 2PC(6), whilst no such an assignment occurs in the scanings. It follows from the theory for intramolecular bicompartamental systems with added quencher<sup>6</sup> that the two quenching rates have to fulfil the following two conditions:

$$k_{Q1} + k_{Q2} = d_1 \quad (12a)$$

$$k_{Q1}k_{Q2} = d_2 \quad (12b)$$

where  $d_1$  and  $d_2$  are constants. Assigning values to  $d_1$  and  $d_2$  from the fitting (Table 3) allows a more thorough investigation of the behavior of the rate constants for quenching. The results for the part of  $k_{Qi}$  space of interest, i.e.,  $1 \times 10^7 \text{ M}^{-1} \text{ s}^{-1} < k_{Qi} < 1 \times 10^8 \text{ M}^{-1} \text{ s}^{-1}$ , are shown graphically in Figure 11. The straight line (eq 12a) and the hyperbole (eq 12b) have two intersection points, which are mutually exchangeable. These two  $k_{Qi}$  pairs correspond to the values found in the scanings and the fittings. Furthermore, the difference between the straight line and the hyperbole is very small over an extended region in  $k_{Qi}$  space. If one does not assign  $k_{Q1}$  to the quenching rate constant  $k_q$  for 2PC(6), the bicompartamental model cannot distinguish between the two theoretically equivalent sets of quenching rate constants (Figure 3 and Table 3).

The importance of the close proximity between the straight line and hyperbole in Figure 11 is clearly demonstrated when the statistical parameter  $\chi_v^2$  resulting from a two-dimensional scan of  $k_{Qi}$  space is plotted as a function of  $k_{Q1}$  and  $k_{Q2}$  (Figure 12). This scan was performed in the region  $1 \times 10^7$  to  $1 \times 10^8 \text{ M}^{-1} \text{ s}^{-1}$  for both constants, comprising the results obtained from the scanning and fitting. The rate constants  $k_{01}$ ,  $k_{21}$ ,  $k_{02}$ , and  $k_{12}$  and the spectral emission parameters  $\tilde{c}_1$  were held constant at the values found in Table 3, whilst the normalized

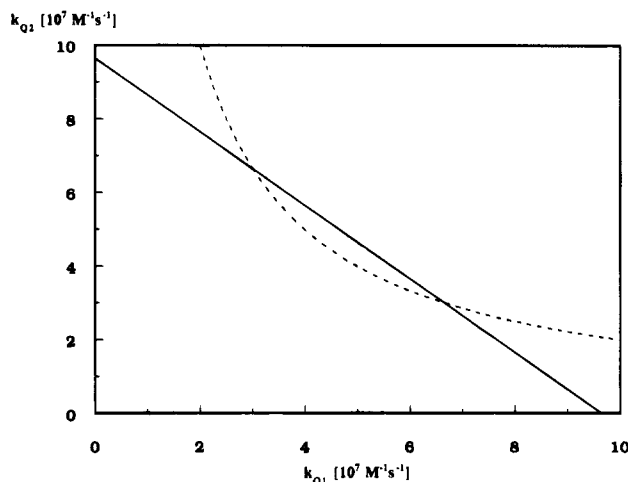


**Figure 11.** The straight line corresponding to eq 12a and the hyperbola corresponding to eq 12b for values of the constants  $d_1$  and  $d_2$  as obtained from the results presented in Table 3a.

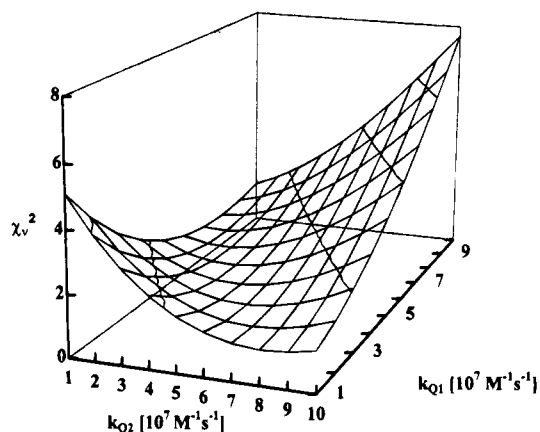


**Figure 12.** Global  $\chi_v^2$ -surfaces from two-dimensional scanings of  $k_{Q1}$  and  $k_{Q2}$ . The contour lines are given at  $\chi_v^2 = 2, 4$ , and  $6$ .

absorbance  $\tilde{b}_1$  was freely adjustable. The two quenching rate constants were held constant at preset values in combinations to cover the  $k_Q$  space scanned. The  $\chi_v^2$  surface shows a very shallow minimum and the whole surface has the form of a valley whose bottom corresponds perfectly to the straight line from eq 12a. Thus, for this particular system, the sum of the rate constants for quenching is more significant than their product for their estimation.

While scanning the pairs of quenching rate constants, it was

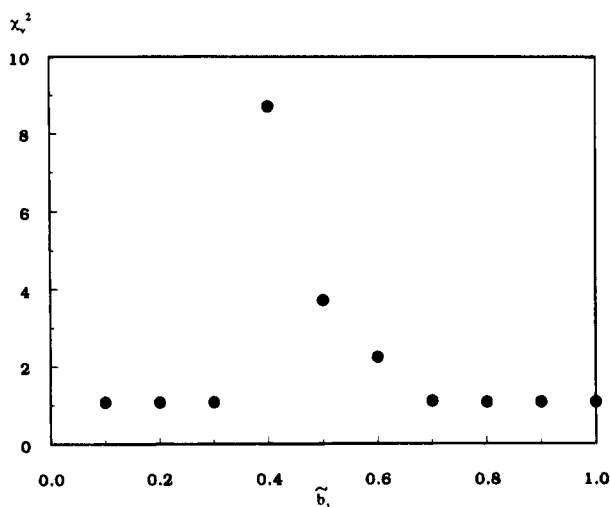


Figure 13. Global  $\chi_v^2$  surface from the scannings of  $\tilde{b}_1$ .

found that the normalized absorbance  $\tilde{b}_1$  took almost the same values over a huge region of the examined  $k_Q$  space. When the scanning already discussed in section 4.1 was performed, however, it was found that the resulting values of  $\tilde{b}_1$  strongly depend on the initial starting values for the computer calculations. To examine the sensitivity to  $\tilde{b}_1$ , the bichromophoric system with added quencher was analyzed at different preset values of  $\tilde{b}_1$  with all other parameters freely adjustable. The resulting  $\chi_v^2$  values as a function of  $\tilde{b}_1$  are shown in Figure 13. Indeed, for  $0.7 \leq \tilde{b}_1 \leq 1$  very good fits were obtained. The good statistics obtained in the region  $0.1 \leq \tilde{b}_1 \leq 0.3$  stems from the fact that compartments 1 and 2 interchange in this region, i.e.,  $\tilde{b}_1$  becomes  $\tilde{b}_2$ .

The parameter values from the fittings following strategy I can be used to construct the SAEMS presented in Figure 14a. First, and most striking, is that the SAEMS obtained from this fitting differ significantly from the ones obtained by scanning, i.e., without the use of a model compound (Figure 4b). In the latter case, it was concluded that the obtained SAEMS did not describe the steady-state spectra well at longer wavelengths: a problem that is absent when the results with the model compound included are used. Indeed, with the model compound included the SAEMS for the locally excited state show no emission at longer wavelengths, which is in agreement with the steady-state spectra in Figure 10. The excimer emission at shorter wavelengths, however, is still unsatisfactorily high.

**4.2.2. Strategy II:**  $k_{01}$  and  $k_{Q1}$  for 2PC(6)2PC Linked with  $k_0$  and  $k_q$  for 2PC(6), Respectively.  $\tilde{c}_1(395 \text{ nm})$  Held Constant at Unity. The results from a fit where the stationary spectral information ( $\tilde{c}_1(395 \text{ nm}) = 1$ ) was included in the fitting are summarized in Table 4. The results for the rate constants  $k_{ij}$  conform with the previous ones, but following strategy II resulted in lower uncertainties compared with those when no stationary spectral information was included (Table 3). Furthermore, the spectral parameters  $\tilde{c}_i$  take much higher values at shorter wavelengths when the stationary spectral information is included. This is important, as the SAEMS obtained when following strategy II (Figure 14b) show much lower excimer emission at shorter wavelengths, which is in better agreement with the steady-state spectra shown in Figure 10. Compared with the previously presented SAEMS, it is only when using a model compound and including stationary spectral information in the fittings that SAEMS are obtained which conform with the steady-state fluorescence spectra given in Figure 10. The value obtained for  $k_{Q1}$  (Table 4) is identical with that obtained via strategy I (Table 3). Thus, the linking of  $k_{Q1}$  and  $k_q$  forces

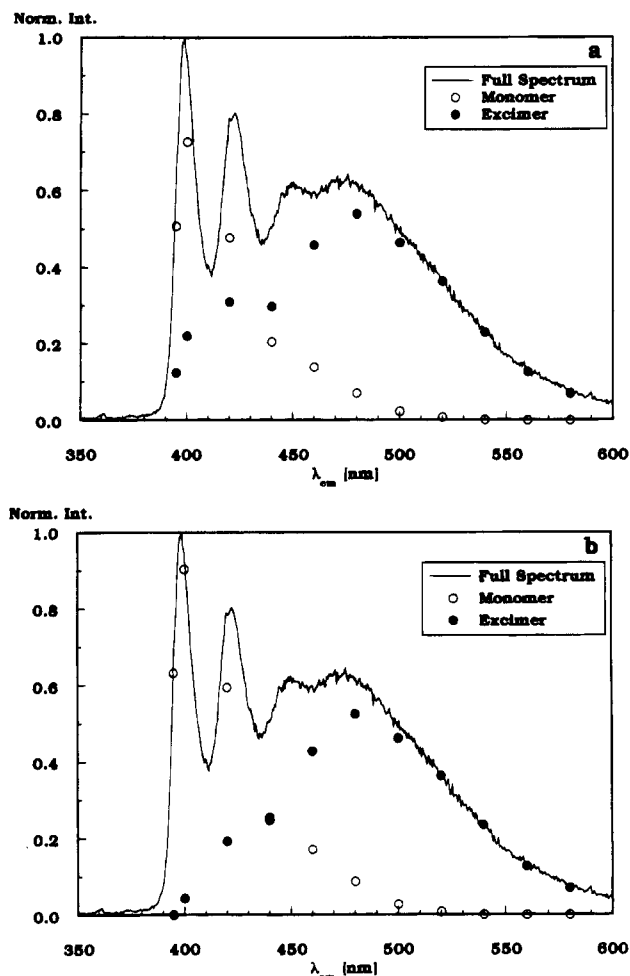


Figure 14. (a) Calculated SAEMS for the locally excited state and excimer emission of 2PC(6)2PC in toluene from the fit following strategy I (see text for details) of the compartmental model to the decay data from the bichromophoric system with added quencher iodo-methane. (b) Calculated SAEMS for the locally excited state and excimer emission of 2PC(6)2PC in toluene from the fit following strategy II (see text for details) of the compartmental model to the decay data from the bichromophoric system with added quencher iodo-methane.

$k_{Q1}$  to take the value of  $k_q$  irrespective of inclusion of stationary spectral information.

**4.3. Decay Surface of 2PC(6)2PC without Added Quencher.** When data from measurements without added quencher are analyzed, three parameters used in the fittings have to be known for identifiability reasons.<sup>5</sup> With no *a priori* knowledge of the system, some assumptions have to be made. For an adequate model compound one can assume that the measured  $k_0$  (eq 11) equals  $k_{01}$  of 2PC(6)2PC. In order to obtain the remaining parameters, a distribution between the two compartments in the ground-state may be assumed or determined by other spectroscopic methods, e.g., NMR,<sup>22</sup> allowing determination of the normalized absorbance  $\tilde{b}_1$ . Furthermore, there may be emission wavelengths where only one of the excited states emits, as is the case for 2PC(6)2PC. Monitoring the emission at one or more of these wavelengths allows the assumption of unity for the value for  $\tilde{c}_i$  at these particular emission wavelengths. For the present system there is an appropriate model compound, but no assumption can be made from time-resolved fluorescence data for the value of  $\tilde{b}_1$  as the previous analysis has clearly shown.

The decay data of a similar bichromophore, 1,3-di(2-pyrenyl)propane in methylcyclohexane, have been analyzed using the

TABLE 4: Analogous Results to Those Presented in Table 3, but for a Global Fit following Strategy II (See Text for Details)

Globally Linked Parameters									
$k_{01}$	$k_{21}$	$k_{01}$	$k_{02}$	$k_{12}$	$k_{Q2}$	$\tilde{b}_1$	$S_1$	$S_2$	P
$0.01826 \pm 2 \times 10^{-5}$	$0.2370 \pm 7 \times 10^{-4}$	$0.0664 \pm 3 \times 10^{-4}$	$0.0881 \pm 2 \times 10^{-4}$	$0.1490 \pm 6 \times 10^{-4}$	$0.0234 \pm 4 \times 10^{-4}$	$0.846 \pm 0.002$	0.256	0.237	0.0353
$Z_{\chi^2}$ 9.93									
Regionally Linked Parameters									
$\lambda_{\text{cm}}$					$\tilde{c}_1$				
I									
395					500	$0.07 \pm 0.06$			
400	$0.957 \pm 0.002$				520	$0.03 \pm 0.07$			
420	$0.768 \pm 0.002$				540	$0.01 \pm 0.07$			
440	$0.525 \pm 0.001$				560	$0.00 \pm 0.07$			
460	$0.302 \pm 0.002$				580	$0.00 \pm 0.07$			
480	$0.151 \pm 0.002$								

method mentioned above,<sup>16</sup> implicitly assuming  $\tilde{c}_1 = 1$  and using a known  $k_{01}$ , e.g., as determined from an adequate model compound, and setting  $\tilde{b}_1 = 1$  (concluded from the same type of analysis as in Figure 6). Applying this method to the fluorescence decay data of 2PC(6)2PC in toluene gives values for the rate constants  $k_{21}$ ,  $k_{02}$ , and  $k_{12}$  which agree with those presented in Table 4, although for 2PC(6)2PC in toluene  $\tilde{b}_1 = 0.85$  at room temperature.

## 5. Conclusions

In this work, the previously presented compartmental models for intramolecular two-state excited-state processes with added quencher<sup>5,6</sup> are for the first time experimentally investigated by time-resolved fluorescence. Such systems are identifiable when one of the rate constants ( $k_{01}$ ,  $k_{21}$ ,  $k_{02}$ , and  $k_{12}$ ) is known. The use of an added quencher is essential if no *a priori* information is available. In the absence of data for the system with added quencher, the system can only be unraveled by the use of *a priori* information, e.g., one of the rate constants has to be known together with  $\tilde{b}_1$  and  $\tilde{c}_1$ .

Two different strategies in the data analysis were followed: one where no steady-state fluorescence information was included in the analysis and one which made use of such information. It turned out that only when stationary spectral information was enclosed were the species-associated emission spectra superimposable with steady-state fluorescence spectra.

The system with added quencher and one known rate constant is fully identifiable. Even for a situation when no *a priori* information is available, the compartmental model can be used to obtain information on a bicompartamental system. By scanning the rate constant  $k_{01}$ , it was possible to obtain physically acceptable upper and lower limits for the rate constants  $k_{01}$ ,  $k_{21}$ ,  $k_{02}$ , and  $k_{12}$ . Including decay traces of quenched 2PC(6) in the data analysis and linking  $k_{01}$  and  $k_{Q1}$  with  $k_0$  and  $k_q$ , respectively, enabled these parameter values to be defined.

The quenching rate constants  $k_{Q1}$  and  $k_{Q2}$  are theoretically determined by eqs 12. For the present system, however, these equations take similar values in the physical range of  $k_{Q1}$ . This leads to imprecise estimates for those rate constants. Only when decay traces from a quenched model compound were included in the global fittings and  $k_{Q1}$  was linked with  $k_q$  does  $k_{Q1}$  take the value of  $k_q$ . This suggests that further investigations on the influence of the values of  $k_{Q1}$  and the extent of quenching are necessary in order to clearly assess the reliability of the obtained parameters of the global compartmental analysis.

**Acknowledgment.** J.v.S. is a postdoctoral fellow at the Katholieke Universiteit Leuven, sponsored by fellowships from IUAP-II-16 and The Swedish Natural Science Research Council through the European Human Capital and Mobility Scheme. J.v.S. also thanks JCH, Sweden, for invaluable support. L.V.D. thanks K.U. Leuven and IUAP-II-16 for financial support. N.B. is an Onderzoeksleider of the Belgian Fonds voor Geneeskundig Wetenschappelijk Onderzoek (FGWO). The continuing support of the Belgian Fonds voor Kollektief Fundamenteel Onderzoek (FKFO) is gratefully acknowledged. Dr. Bart Hermans is thanked for fruitful discussions, Dr. Johan Hofkens and Mrs. Sigrid Depaemelaere are thanked for the maintenance of the single-photon timing systems, and Dr. Wolfgang Kühnle is thanked for the synthesis of 2PC(6)2PC and 2PC(6).

## References and Notes

- (1) Ameloot, M.; Boens, N.; Andriessen, R.; Van den Bergh, V.; De Schryver, F. C. J. *Phys. Chem.* **1991**, *95*, 2041.

- (2) Andriessen, R.; Boens, N.; Ameloot, M.; De Schryver, F. C. *J. Phys. Chem.* **1991**, 95, 2047.
- (3) Andriessen, R.; Ameloot, M.; Boens, N.; De Schryver, F. C. *J. Phys. Chem.* **1992**, 96, 314.
- (4) (a) Beechem, J. M.; Ameloot, M.; Brand, L. *Chem. Phys. Lett.* **1985**, 120, 466. (b) Ameloot, M.; Beechem, J. M.; Brand, L. *Chem. Phys. Lett.* **1986**, 129, 211.
- (5) Boens, N.; Andriessen, R.; Ameloot, M.; Van Dommelen, L.; De Schryver, F. C. *J. Phys. Chem.* **1992**, 96, 6331.
- (6) Boens, N.; Ameloot, M.; Hermans, B.; De Schryver, F. C.; Andriessen, R. *J. Phys. Chem.* **1993**, 97, 799.
- (7) Boens, N.; Van Dommelen, L.; Ameloot, M. *Biophys. Chem.* **1993**, 48, 301.
- (8) Van Dommelen, L.; Boens, N.; Ameloot, M.; De Schryver, F. C.; Kowalczyk, A. *J. Phys. Chem.* **1993**, 97, 11738.
- (9) Boens, N.; Van Dommelen, L.; De Schryver, F. C.; Ameloot, M. *Time-Resolved Laser Spectroscopy in Biochemistry IV*, Proceedings of SPIE—The International Society for Optical Engineering; Lakowicz, J. R., Ed.; SPIE—The International Society for Optical Engineering: Bellingham, WA, 1994; Vol. 2137, p 400.
- (10) (a) Knutson, J. R.; Beechem, J. M.; Brand, L. *Chem. Phys. Lett.* **1983**, 102, 501. (b) Beechem, J. M.; Knutson, J. R.; Brand, L. *Photochem. Photobiol.* **1983**, 37, abstr. S20. (c) Beechem, J. M.; Ameloot, M.; Brand, L. *Anal. Instrum.* **1985**, 14, 379.
- (11) (a) Striker, G. In *Deconvolution and Reconvolution of Analytical Signals*; Bouchy, M., Ed.; University Press: Nancy, 1982; p 329. (b) Zachariasse, K. A.; Duveneck, G.; Kühnle, W.; Reynders, P.; Striker, G. *Chem. Phys. Lett.* **1987**, 133, 390.
- (12) (a) Löfroth, J.-E. *Anal. Instrum.* **1985**, 14, 403. (b) Löfroth, J.-E. *Eur. Biophys. J.* **1985**, 13, 45.
- (13) (a) Boens, N.; Janssens, L. D.; De Schryver, F. C. *Biophys. Chem.* **1989**, 33, 77. (b) Janssens, L. D.; Boens, N.; Ameloot, M.; De Schryver, F. C. *J. Phys. Chem.* **1990**, 94, 3564.
- (14) Löfroth, J.-E. *J. Phys. Chem.* **1986**, 90, 1160.
- (15) Reynders, P.; Kühnle, W.; Zachariasse, K. A. *J. Am. Chem. Soc.* **1990**, 112, 3929.
- (16) Zachariasse, K. A.; Duveneck, G.; Kühnle, W. *Chem. Phys. Lett.* **1985**, 113, 337.
- (17) (a) Boens, N.; Van den Zegel, M.; De Schryver, F. C.; Desie, G. In *From Photophysics to Photobiology*; Favre, A., Tyrell, R., Cadet, J., Eds.; Elsevier: Amsterdam, 1987; p 93. (b) Khalil, M. M. H.; Boens, N.; Van der Auweraer, M.; Ameloot, M.; Andriessen, R.; Hofkens, J.; De Schryver, F. C. *J. Phys. Chem.* **1991**, 95, 9375.
- (18) (a) Gauduchon, P.; Wahl, Ph. *Biophys. Chem.* **1978**, 8, 87. (b) Wijnaendts van Resandt, R. W.; Vogel, R. H.; Provencher, S. W. *Rev. Sci. Instrum.* **1982**, 53, 1392. (c) Zuker, M.; Szabo, A. G.; Bramall, L.; Krajcarski, D. T.; Selinger, B. *Rev. Sci. Instrum.* **1985**, 56, 14. (d) Boens, N.; Ameloot, M.; Yamazaki, I.; De Schryver, F. C. *Chem. Phys.* **1988**, 121, 73.
- (19) Marquardt, D. W. *J. Soc. Ind. Appl. Math.* **1963**, 11, 431.
- (20) Boens, N. In *Luminescence Techniques in Chemical and Biochemical Analysis*; Baeyens, W. R. G., De Keukeleire, D., Korkidis, K., Eds.; Marcel Dekker: New York, 1991; pp 21.
- (21) (a) Lakowicz, J. R.; Johnson, M. L.; Joshi, N.; Gryczynski, I.; Laczko, G. *Chem. Phys. Lett.* **1986**, 131, 343. (b) Lakowicz, J. R.; Kusba, J.; Szmecinski, H.; Johnson, M. L.; Gryczynski, I. *Chem. Phys. Lett.* **1993**, 206, 455.
- (22) Reynders, P.; Dreeskamp, H.; Kühnle, W.; Zachariasse, K. A. *J. Phys. Chem.* **1987**, 91, 3982.

JP942695U